

Extensions of sub-Nyquist Radar: Reduced Time-on-Target and Cognitive Radar

Deborah Cohen, Alex Dikopoltsev, Yonina C. Eldar
Technion - Israel Institute of Technology, Haifa, Israel
{debby@tx, salexd@t2, yonina@ee}.technion.ac.il

Abstract—Pulse Doppler radars measure both the targets distance to the transceiver and their radial velocity, through the estimation of the time delays and Doppler frequencies, respectively. This digital processing is traditionally performed on samples of the received signal at its Nyquist rate, which can be prohibitively high. Overcoming the rate bottleneck, sub-Nyquist sampling methods have been proposed that break the link between radar signal bandwidth and sampling rate. In this work, we extend these methods in two directions. First, we allow for a reduced time-on-target by transmitting non-uniformly spaced pulses. Second, we pave the way to sub-Nyquist cognitive radar by considering transmitted and received pulses with dynamic support composed of several narrow bands. Both software and hardware simulations demonstrate reduced time-on-target and dynamic transmitted signal support.

I. INTRODUCTION

Radar is a remote-sensing system widely used for both military and civilian purposes. In this work, we focus on pulse Doppler radar, which emits a periodic series of pulses; the pulse-to-pulse interval is referred to as the pulse repetition interval (PRI). Following the Swerling-0 model [1], targets are non-fluctuating point targets, sparsely populated in the radar unambiguous time-frequency region: delays up to the PRI and Doppler frequencies up to its reciprocal. After reflecting off the targets, the pulses propagate back to the receiver. We consider a monostatic radar, composed of a single transceiver, that is the transmitter and receiver are collocated.

Classic radar processing [1], [2] samples and processes the received signal at its Nyquist rate. A traditional receiver is composed of either an analog matched filter (MF) followed by a high rate analog to digital converter (ADC) or in modern systems, an ADC followed by a digital MF. Spectral analysis is then conducted along the slow time dimension, namely across the pulses, typically using the digital Fourier transform (DFT). The pulse Doppler processing results in a data matrix in which the dimensions are fast time and Doppler frequency, or delay-Doppler map. Detection processes, such as peak detection, can then be performed on the recovered map.

Unfortunately, Nyquist frequencies of radar signals can be very high, up to hundreds of MHz or even several GHz. Such high sampling rates generate a large number of samples to process, affecting speed and power consumption. To overcome the rate bottleneck, new sampling methods have recently been

proposed that break the link between radar signal bandwidth and sampling rate [3], [4], [5]. The sub-Nyquist Xampling ("compressed sampling") [6] method used is an ADC which performs analog prefiltering of the signal before taking point-wise samples. The compressed samples, or "Xamples", contain the information needed to recover the desired signal parameters using compressed sensing (CS) algorithms.

In [3], sub-Nyquist sampling and delay recovery techniques are presented, along with the design and implementation of a corresponding hardware prototype. The authors in [4], [5] expand both the theoretical algorithm and hardware prototype from [3] to include Doppler frequency recovery. In [4], a two-stage recovery technique separates delay and Doppler estimation, performing them sequentially rather than in parallel, while in [5], both delays and Doppler frequencies are estimated simultaneously, leading to increased signal to noise ratio (SNR). The authors' approach in [5], referred to as Doppler focusing, combines the received signals from different pulses, for any Doppler frequency, so that targets with appropriate Doppler frequencies come together in phase. For each frequency, a simple one-dimensional CS problem is obtained and the appropriate delays are recovered.

Several additional works apply CS techniques to radar, but do not address sampling rate reduction and still sample the received signal at the Nyquist rate [7], [8]. In [7], the delay-Doppler plane is discretized and a CS dictionary with a column for each two dimensional grid point is constructed. The main drawback of this approach is the prohibitive dictionary size for any realistic scenario in terms of memory, processing time and computational complexity. Avoiding this issue, the authors in [8] adopt a two-step approach, where they first estimate the delays and then use these to recover the corresponding Doppler frequencies and amplitudes. Again, this two-stage recovery approach, which does not benefit from coherent superposition of the different pulses, does not handle noise well. In [9], a sub-Nyquist approach is considered, that only recovers delays and does not treat noise.

In this work, we adopt the approach in [3], [5] for pulse Doppler radar and propose two main extensions: reduced time-on-target and cognitive radar (CR) [10]. When considering a directional antenna, in order to be able to distinguish between targets located in different directions, the time-on-target, namely the time needed for discovering a target in a specific direction, is the coherent processing interval (CPI), which is equal to the product of the number of transmitted pulses P and the PRI. The resolution in Doppler frequency is governed by P , which leads to a trade-off between large P for high resolution and small P for short time-on-target. We propose to send the P pulses non-uniformly and exploit the periods of time where no pulse is sent to a specific direction to

This work is supported in part by the Semiconductor Research Corporation (SRC) through the Texas Analog Center of Excellence (TxACE) at the University of Texas at Dallas (Task ID:1836.114), in part by the Israel Science Foundation under Grant no. 170/10, in part by the Ollendorf foundation, and in part by the Intel Collaborative Research Institute for Computational Intelligence (ICRI-CI). Deborah Cohen is grateful to the Azrieli Foundation for the award of an Azrieli Fellowship.

send a pulse to another one. This way, we can deal with several directions during the same CPI, reducing the overall time-on-target. To process the received signal, we combine Xampling with matrix sketching [11].

In order to increase the flexibility and responsiveness of the sub-Nyquist pulse radar prototype described in [3], [5], we consider the CR approach. Haykin [10] defines CR as a radar system with adaptive transmission and reception capabilities, namely both the transmitter and receiver are able to dynamically adjust to the environment conditions. Here, we extend the sub-Nyquist pulse Doppler radar to allow for transmission and reception of several narrow frequency bands, rather than a wideband spectrum. To comply with CR requirements, the bands support vary with time to allow for dynamic adaptation to the environment. Moreover, such a system allows us to disguise the transmitted signal or cope with overloaded spectrum by using a smaller portion of it.

This paper is organized as follows. In Section II, we present the radar model and the assumptions used for simplification. Section III introduces the reduced time-on-target approach based on non-uniform pulses. In Section IV, we describe our modified sub-Nyquist pulse radar prototype in the context of CR. Numerical experiments are presented in Section V.

II. STANDARD RADAR MODEL AND GOAL

Consider a standard pulse-Doppler radar transceiver that transmits a pulse train

$$x_T(t) = \sum_{p=0}^{P-1} h(t - p\tau), \quad 0 \leq t \leq P\tau, \quad (1)$$

consisting of P equally spaced pulses $h(t)$. The pulse-to-pulse delay τ is the PRI, and its reciprocal $1/\tau$ is the pulse repetition frequency (PRF). The entire span of the signal in (1) is called the CPI. The pulse $h(t)$ is a known time-limited baseband function with continuous-time Fourier transform (CTFT) $H(\omega) = \int_{-\infty}^{\infty} h(t)e^{-j\omega t} dt$. We assume that $H(\omega)$ has negligible energy at frequencies beyond $B_h/2$ and we refer to B_h as the bandwidth of $h(t)$.

Now, consider L non-fluctuating point-targets, according to the Swerling-0 model [1], where L , or at least an upper bound for it, is assumed to be known. The pulses reflect off the L targets and propagate back to the transceiver. The l th target is defined by three parameters: a time delay τ_l , proportional to the target distance to the radar; a Doppler radial frequency ν_l , proportional to the target closing velocity to the radar; and a complex amplitude α_l , proportional to the target radar cross section, dispersion attenuation and other propagation factors. The targets are defined in the radar radial coordinate system and assumed to lie in the radar unambiguous time-frequency region: delays up to the PRI and Doppler frequencies up to the PRF. Besides, we make the following assumptions on the targets location and motion, leading to a simplified expression of the received signal:

- A1** "Far targets" - assuming the target distance to the radar is large compared to the distance change during the CPI, namely α_l is constant.
- A2** "Slow targets" - assuming the target velocity is small enough to allow for constant τ_l during the CPI.

- A3** "Small Acceleration" - assuming the target velocity remains approximately constant during the CPI, namely ν_l is constant.

In these conditions, the received signal can be written as

$$x(t) = \sum_{p=0}^{P-1} \sum_{l=0}^{L-1} \alpha_l h(t - \tau_l - p\tau) e^{-j\nu_l p\tau}, \quad 0 \leq t \leq P\tau. \quad (2)$$

It will be convenient to express $x(t)$ as a sum of single frames

$$x(t) = \sum_{p=0}^{P-1} x_p(t), \quad (3)$$

where

$$x_p(t) = \sum_{l=0}^{L-1} \alpha_l h(t - \tau_l - p\tau) e^{-j\nu_l p\tau}, \quad 0 \leq t \leq P\tau. \quad (4)$$

Consider the Fourier series representation of the aligned frames $x_p(t + m_p\tau)$:

$$X_p[k] = \frac{1}{\tau} H[k] \sum_{l=0}^{L-1} \alpha_l e^{-j2\pi k\tau_l/\tau} e^{-j\nu_l p\tau}, \quad 0 \leq k \leq N-1. \quad (5)$$

From (5), we see that the unknown parameters $\{\alpha_l, \tau_l, \nu_l\}_{l=0}^{L-1}$ are embodied in the Fourier coefficients $X_p[k]$. The goal is then to recover these parameters from $X_p[k]$.

III. REDUCED TIME-ON-TARGET

A. Motivation

The resolution in Doppler frequency in standard processing is governed by P . More precisely, it is equal to $2\pi/P\tau$. However, a large P leads to large CPI and large time-on-target. In this work, we wish to break the relation between CPI and time-on-target. To that end, we propose to keep P small but increase resolution by sending the P pulses non-uniformly, namely allowing for non-uniform time steps between the pulses. This way, we can keep the same CPI but still send a smaller number of pulses, reducing power consumption. In addition, the periods of time where no pulse is transmitted in a certain direction can be exploited to send pulses in others, reducing the average time-on-target. In this section, we describe how a delay-Doppler map can be recovered from non-uniform pulses, for one direction, without loss of resolution. In the simulations, we show that 4 directions can be scanned in a single CPI.

B. Xampling with Non-Uniform Pulses

Suppose that the p th pulse is sent at time $m_p\tau$, where $\{m_p\}_{p=0}^{P-1}$ is an ordered set of integers satisfying $m_p \geq p$. In this case, (1) becomes

$$x_T(t) = \sum_{p=0}^{P-1} h(t - m_p\tau), \quad 0 \leq t \leq P\tau, \quad (6)$$

(3) still holds, (4) and (5) change to

$$x_p(t) = \sum_{l=0}^{L-1} \alpha_l h(t - \tau_l - m_p\tau) e^{-j\nu_l m_p\tau}, \quad 0 \leq t \leq P\tau, \quad (7)$$

and

$$X_p[k] = \frac{1}{\tau} H[k] \sum_{l=0}^{L-1} \alpha_l e^{-j2\pi k \tau_l / \tau} e^{-j\nu_l m_p \tau}, \quad 0 \leq k \leq N-1, \quad (8)$$

respectively. We use the same sub-Nyquist sampling scheme as in [3], [5], where it is shown how we can compute $X_p[k]$ for some chosen k from the "Xamples". In the next sections, we show how the processing with uniform pulses can be extended in order to recover the delays and Doppler frequencies in the non-uniform case.

C. Delay-Doppler Recovery Conditions

Suppose that we limit ourselves to the Nyquist grid so that $\tau_l/\tau = s_l/N$, where s_l is an integer satisfying $0 \leq s_l \leq N-1$, and $\nu_l \tau = 2\pi r_l/M$, where r_l is an integer in the range $0 \leq r_l \leq M-1$.

Let \mathbf{X} be the $K \times P$ matrix with p th column given by $X_p[k]$. We can then write \mathbf{X} as

$$\mathbf{X} = \mathbf{H} \mathbf{F}_N^K \mathbf{A} (\mathbf{F}_M^P)^T. \quad (9)$$

Here $\mathbf{H} = \frac{1}{\tau} \text{diag}(H[k])$, \mathbf{F}_N^K denotes K rows from the $N \times N$ Fourier matrix, corresponding to the K selected Fourier coefficients, and \mathbf{F}_M^P denotes P rows from the $M \times M$ Fourier matrix, indexed by the values of $m_p, 1 \leq p \leq P$. When sampling at the Nyquist rate, $K = N$ and \mathbf{F}_N is the standard $N \times N$ Fourier matrix. When considering sub-Nyquist sampling, $K < N$. Similarly, when considering uniformly spaced pulses $P = M$ and \mathbf{F}_M is the standard $M \times M$ matrix. When considering non-uniform pulses, $P < M$. The matrix \mathbf{A} is an $N \times M$ sparse matrix that contains the value α_l at the L indices $\{s_l, r_l\}$. The goal is to recover \mathbf{A} from the $K \times P$ matrix \mathbf{X} .

To this end, we use CS algorithms to recover the sparse matrix \mathbf{A} from the measurement matrix \mathbf{X} . We first consider

$$\mathbf{Y} = \mathbf{H}^{-1} \mathbf{X} \quad (10)$$

and obtain

$$\mathbf{Y} = \mathbf{U} \mathbf{A} \mathbf{V}, \quad (11)$$

where $\mathbf{U} \triangleq \mathbf{F}_N^K$ and $\mathbf{V} \triangleq (\mathbf{F}_M^P)^T$.

The following theorem derives a necessary condition on the minimal number of samples K and pulses P for perfect recovery in a noiseless environment.

Theorem 1. *The minimal number of samples required for perfect recovery of \mathbf{A} with L targets in a noiseless environment is $4L^2$, with $K \geq 2L$ and $P \geq 2L$.*

Proof: The observation model (11) can be equivalently written in vector form using the Kronecker product as

$$\text{vec}(\mathbf{Y}) = (\mathbf{V}^T \otimes \mathbf{U}) \text{vec}(\mathbf{A}). \quad (12)$$

Here $\text{vec}(\mathbf{A})$ is a column vector that vectorizes the matrix \mathbf{A} by stacking its columns and \otimes denotes the Kronecker product. It follows that $\text{vec}(\mathbf{A})$ is L -sparse, as well as \mathbf{A} . In order to recover $\text{vec}(\mathbf{A})$ from $\text{vec}(\mathbf{Y})$, we require [12]

$$\text{spark}(\mathbf{V}^T \otimes \mathbf{U}) > 2L. \quad (13)$$

From [13] (Theorem 3.1), it holds that

$$\text{spark}(\mathbf{V}^T \otimes \mathbf{U}) = \min\{\text{spark}(\mathbf{V}^T), \text{spark}(\mathbf{U})\} \quad (14)$$

Therefore, we require both

$$\text{spark}(\mathbf{U}) > 2L \quad (15)$$

$$\text{spark}(\mathbf{V}) > 2L, \quad (16)$$

which in turn leads to both $K \geq 2L$ and $P \geq 2L$. ■

We note that this result was previously proved in [5] in the context of pulse Doppler radar with uniform pulses.

D. Delay-Doppler Recovery

To recover the sparse matrix \mathbf{A} , we solve the following optimization problem [11]

$$\min \|\mathbf{A}\|_1 \text{ s.t. } \mathbf{U} \mathbf{A} \mathbf{V} = \mathbf{Y}, \quad (17)$$

where $\|\mathbf{A}\|_1 = \sum_{i,j} |A_{ij}|$ is the ℓ_1 -norm of $\text{vec}(\mathbf{A})$. In [11], the authors consider a greedy based approach which extends the standard OMP to matrix form to solve (17), as shown in Algorithm 1.

Algorithm 1 OMP for sparse matrix recovery [11]

Input: observation matrix \mathbf{Y} , measurement matrices \mathbf{U} , \mathbf{V}
Output: index set Λ containing the locations of the non zero indices of \mathbf{A} , estimate for signal matrix $\hat{\mathbf{A}}$

- 1: Initialization: residual $\mathbf{R}_0 = \mathbf{Y}$, index set $\Lambda_0 = \emptyset$, $t = 0$
- 2: Find the two indices $\lambda_t = [\lambda_t(1) \quad \lambda_t(2)]$ such that

$$[\lambda_t(1) \quad \lambda_t(2)] = \arg \max_{i,j} |\mathbf{v}_j^T \mathbf{R}_{t-1}^T \mathbf{u}_i|$$

- 3: Augment index set $\Lambda_t = \Lambda_t \cup \{\lambda_t\}$
- 4: Find the new signal estimate

$$\mathbf{a}_t = \mathbf{D}_t^{-1} \mathbf{d}_t$$

where \mathbf{D}_t and \mathbf{d}_t are defined below

- 5: Compute new residual

$$\mathbf{R}_t = \mathbf{Y} - \sum_{m=1}^t \mathbf{a}_t(m) \mathbf{u}_{\lambda_t(m,1)} \mathbf{v}_{\lambda_t(m,2)}^T$$

- 6: Increment t and return to step 2 if $t \leq L$, otherwise stop
 - 7: Estimated support set $\hat{\Lambda} = \Lambda_L$
 - 8: Estimated signal matrix $\hat{\mathbf{A}}$: $(\Lambda_L(m,1), \Lambda_L(m,1))$ -th component of $\hat{\mathbf{A}}$ is given by $\mathbf{a}_L(m)$ for $m = 1, \dots, L$ while rest of the elements are zeros
-

The following notations are adopted: \mathbf{a}_i^T and \mathbf{a}_j are the i th row and j th column of the matrix \mathbf{A} , respectively. Moreover, \mathbf{D}_t is a $t \times t$ matrix in which the (m, r) -th element is given by

$$(\mathbf{D}_t)_{m,r} = \mathbf{v}_{\lambda_t(r,2)}^T \mathbf{v}_{\lambda_t(m,2)} \mathbf{u}_{\lambda_t(m,1)}^T \mathbf{u}_{\lambda_t(r,1)}^T$$

for $m, r = 1, \dots, t$ and

$$\mathbf{d} = [\mathbf{v}_{\lambda_t(1,2)}^T \mathbf{Y}^T \mathbf{u}_{\lambda_t(1,1)} \quad \dots \quad \mathbf{v}_{\lambda_t(t,2)}^T \mathbf{Y}^T \mathbf{u}_{\lambda_t(t,1)}]^T$$

is a $t \times 1$ vector.

With the noisy version of (11), we aim to solve the following ℓ_1 -norm minimization problem

$$\min_{\mathbf{A}} \left\{ \frac{1}{2} \|\mathbf{Y} - \mathbf{U} \mathbf{A} \mathbf{V}\|_F^2 + \lambda \|\mathbf{A}\|_1 \right\}, \quad (18)$$

where λ is a regularization parameter and $\|\cdot\|_F$ denotes the Frobenius norm. The authors in [11] extend FISTA to sparse matrix recovery with matrix inputs (see Algorithm 2).

Algorithm 2 FISTA for sparse matrix recovery [11]

Input: observation matrix \mathbf{Y} , measurement matrices \mathbf{U}, \mathbf{V}

Output: estimate for signal matrix $\hat{\mathbf{A}}$

```

1: Initialization:  $\mathbf{A}^0 = \mathbf{0}, \mathbf{A}^1 = \mathbf{0}, t_0 = 1, t_1 = 1, k = 1$ 
2: Initialize:  $\lambda_1, \beta \in (0, 1), \bar{\lambda} > 0$ 
3: while not converged do
4:    $\mathbf{Z}^k = \mathbf{A}^k + \frac{t_{k-1}-1}{t_k} (\mathbf{A}^k - \mathbf{A}^{k-1})$ 
5:    $\mathbf{W}^k = \mathbf{Z}^k - \frac{1}{P} \mathbf{U}^T (\mathbf{U} \mathbf{Z}^k \mathbf{V}^T - \mathbf{Y}) \mathbf{V}$ 
6:    $\mathbf{A}^{k+1} = \text{soft} \left( \mathbf{W}^k, \frac{\lambda_k}{L_f} \right)$ 
7:    $t_{k+1} = \frac{1 + \sqrt{4t_k^2 + 1}}{2}$ 
8:    $\lambda_{k+1} = \max(\beta \lambda_k, \bar{\lambda})$ 
9:    $k = k + 1$ 
end while
10:  $\hat{\mathbf{A}} = \mathbf{A}^k$ 
    
```

In Algorithm 2, $L_f = \|\mathbf{V}^T \otimes \mathbf{U}\|_2$ is the Lipschitz constant of the gradient of $\frac{1}{2} \|\text{vec}(\mathbf{Y}) - (\mathbf{V}^T \otimes \mathbf{U}) \text{vec}(\mathbf{A})\|_2^2$ and

$$\text{soft}(\mathbf{w}, \lambda) = \text{sgn}(\mathbf{w}_i) (|\mathbf{w}_i| - \lambda)_+, \quad (19)$$

for $i = 1, \dots, N^2$ where \mathbf{w}_i is the i th element of \mathbf{w} , x_+ equals x if $x > 0$ and 0 otherwise. In the simulations, we only consider the extended FISTA to recover \mathbf{A} from \mathbf{Y} , due to lack of space.

IV. COGNITIVE RADAR

In this section, we consider a radar pulse whose spectrum is composed of narrow bands, rather than a wideband spectrum and show how we can use our system to allow for a dynamic adaptation of both the transmitted and received signal spectrum, paving the way to CR [10]. We start by discussing the selection of the K Fourier coefficients $X_p[k]$ out of N coefficients. We then briefly describe the radar prototype presented in [3], designed for delay recovery and upgraded in [5] to allow for joint delay and Doppler frequency recovery, and show how we adapted it to CR.

A. Fourier Coefficients Selection

In [5] as well as in Section III-C, it was shown that the number of measured Fourier coefficients K should be at least $2L$. The question of choosing these coefficients is one both theoretical and practical. In [14], the authors analyze the case where the frequency samples are selected uniformly at random. Unfortunately, random frequency sampling is not practical in hardware. Some practical guidelines for choosing the frequencies, suggested in [15], are used in [3] to solve the trade-off between noise robustness, which is increased by highly distributed frequency samples [16], and practical hardware implementation. A multiple bandpass sampling approach was chosen, where four groups of consecutive coefficients are selected. In the next section, we briefly describe our radar prototype [3], [5], and in particular the multiple bandpass frequency sampling.

B. Hardware Prototype

At the heart of our system lies a proprietary developed sub-Nyquist radar receiver board. This analog front-end is fed a synthesized RF signal using National Instruments (NI) hardware. The board is composed of four parallel channels which sample distinct bands of the radar signal spectral content. In each channel, the desired band of bandwidth B_x is filtered, demodulated to baseband and sampled at its Nyquist rate. This way, four sets of consecutive Fourier coefficients are acquired. In the setup from [3], [5], a signal with Nyquist rate 20 MHz is considered. Each channel samples a band with bandwidth $B_x = 80$ KHz at 250 KHz, resulting in an overall sampling rate of 1 MHz, namely 5% of the Nyquist rate. The following combination of four bands was heuristically found to yield good performance: 590-670 KHz; 690-770 KHz; 1315-1395 KHz; 1574-1654KHz. More details on the hardware design can be found in [3]. After sampling, the spectrum of each channel output is computed via fast Fourier transform (FFT) and the 320 Fourier coefficients are used for digital recovery of the delay-Doppler map [5].

C. Paving the Way to Cognitive Radar

We now show how our system can be modified to fit CR requirements and allow for dynamic transmission and reception of several narrow frequency bands. In the setup described above, the transmitter broadcasts a wideband signal, which reflects on the targets and propagates back to the receiver. The received signal is then filtered before sampling, so that only the content of a few narrow bands is sampled and processed. For broadband frequency occupation and power saving, we propose to transmit only the narrow frequency bands that are to be sampled. This will not affect any aspect of the processing since the received signal is preserved in the band of interest. Let $\tilde{H}(\omega)$ be the CTFT of the new transmitted radar pulse,

$$\tilde{H}(\omega) = \begin{cases} H(\omega) & \omega \in [f_x^i - B_x^i/2, f_x^i + B_x^i/2] \text{ for } 1 \leq i \leq N_b \\ 0 & \text{else,} \end{cases} \quad (20)$$

where N_b is the number of filtered bands, B_x^i and f_x^i are the bandwidth and center frequency of the i th band, respectively. Obviously, the computation of the relevant Fourier coefficients $X_p[k]$ will not change. Now, to comply with CR requirements, the bands parameters B_x^i and f_x^i vary with time to allow for dynamic adaptation to the environment. This approach leads to three main advantages. First, the CS reconstruction allows for a better resolution. Second, since we only use the received bands to transmit, the SNR is improved as well. Last, this technique allows for a dynamic form of the transmitted signal spectrum.

V. SIMULATIONS

In this section, we present some numerical experiments illustrating the recovery performance of a sparse target scene.

A. Reduced Time-on-Target

We consider $L = 5$ targets with delays and Doppler frequencies spread uniformly at random in the appropriate unambiguous region, and amplitudes with constant absolute value and random phase. The pulse Doppler radar transmits P pulses with bandwidth $B_n = 200\text{MHz}$ and PRI $\tau = 10\mu\text{sec}$

over a CPI of 1msec, namely $P = 100$ in the uniform case. In the non-uniform approach, we consider $P = 10, 20$ and 50 pulses, chosen uniformly at random. The received signal is corrupted with additive white Gaussian noise (AWGN) $n(t)$ with power spectral density $N_0/2$, bandlimited to B_h . The SNR for the l th target is defined as

$$\text{SNR}_l = \frac{\frac{1}{T_p} \int_0^{T_p} |\alpha_l h(t)|^2 dt}{N_0 B_h}, \quad (21)$$

where T_p is the pulse time. We consider a 1 : 10 sampling rate reduction; we choose $K = 200$ Fourier coefficients per pulse uniformly at random, as opposed to the 2000 Nyquist rate samples per pulse. We use a hit-or-miss criterion as performance metric. A "hit" is defined as a delay-Doppler estimate which is circumscribed by an ellipse around the true target position in the time-frequency plane. We used ellipses with axes equivalent to ± 3 times the time and frequency Nyquist bins. Here, the classic time and frequency resolutions, or Nyquist bins, defined as $1/B_h$ and $1/P\tau$, are 5nsec and 1KHz, respectively. Figure 1 shows the hit rate performance of our recovery method for different values of P and SNR using FISTA. Each experiment is repeated over 100 realisations.

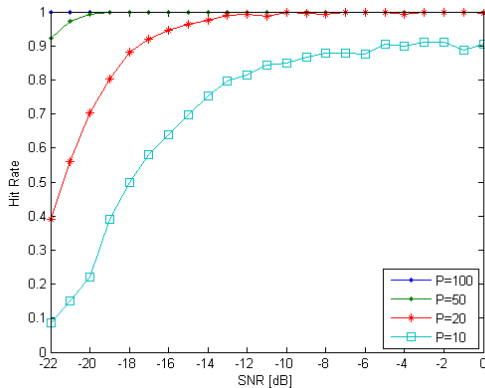


Fig. 1. Influence of the SNR on the hit rate rate with FISTA.

We now show the performance of four delay-Doppler maps recovery. We generate 4 sets of 25 pulses uniformly at random, which are transmitted in 4 different directions. We observe that the performance is similar for all directions, in particular for the first three. as demonstrated in Fig. 2.

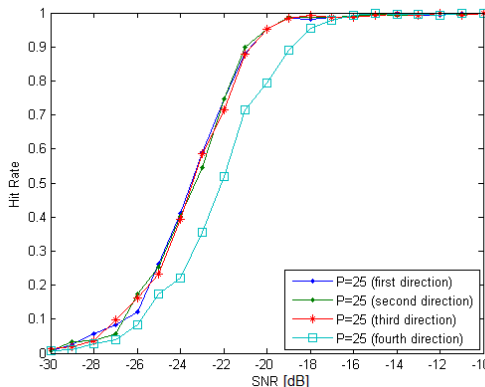


Fig. 2. Four simultaneous delay-Doppler maps recovery in a single CPI.

B. Cognitive Radar

We now consider different scenarios, including closed targets ($L = 3 - 6$) both in terms of delays and Doppler

frequencies. The pulse Doppler radar transmits $P = 100$ pulses with bandwidth $B_h = 10\text{MHz}$, spread over 4 frequency bands each with bandwidth $B_x = 81\text{KHz}$, with PRI $\tau = 1\text{msec}$ and a CPI of 100msec. The received signal is corrupted AWGN as in the previous simulations. Figure 3 shows that our approach, with 4 different combinations of frequency bands, outperforms the case where a signal is sent over the entire wide band, with the same total power.

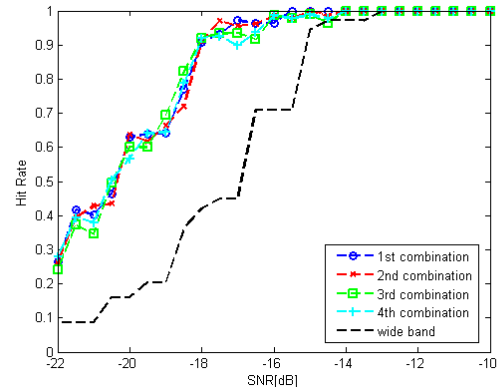


Fig. 3. Delay-Doppler maps recovery with transmitted signal over 4 narrow bands vs. one wideband.

REFERENCES

- [1] M. Skolnik, *Radar handbook*. McGraw Hill, 1970.
- [2] M. A. Richards, *Fundamentals of Radar Signal Processing*. McGraw Hill, 2005.
- [3] E. Baransky, G. Itzhak, I. Shmuel, N. Wagner, E. Shoshan, and Y. C. Eldar, "A sub-Nyquist radar prototype: Hardware and applications," *IEEE Trans. Aerosp. and Elect. Syst.*, vol. 50, pp. 809–822, Apr. 2014.
- [4] O. Bar-Ilan and Y. C. Eldar, "Sub-Nyquist radar," *Int. ITG Conf. Syst., Comm., Coding*, Jan. 2013.
- [5] —, "Sub-Nyquist radar via Doppler focusing," *IEEE Trans. Sig. Proc.*, vol. 62, pp. 1796–1811, Apr. 2014.
- [6] M. Mishali, Y. C. Eldar, and A. J. Elron, "Xampling: Signal acquisition and processing in union of subspaces," *IEEE Trans. Signal Process.*, vol. 59, no. 10, pp. 4719–4734, Oct. 2011.
- [7] M. A. Herman and T. Strohmer, "High-resolution radar via compressed sensing," *IEEE Trans. Sig. Proc.*, vol. 57, pp. 2275–2284, Jun. 2009.
- [8] B. Demissie, "High-resolution range-Doppler imaging by coherent block-sparse estimation," *Int. Work. Comp. Sens. Appl. Radar*, May 2012.
- [9] R. Baraniuk and P. Steeghs, "Compressive radar imaging," *IEEE Radar Conf.*, Apr. 2007.
- [10] S. Haykin, "Cognitive radar - A way of the future," *IEEE Signal Processing Magazine*, vol. 23, pp. 30–40, Jan. 2006.
- [11] T. Wimalajeewa, Y. C. Eldar, and P. K. Varshney, "Recovery of sparse matrices via matrix sketching," *CoRR*, vol. abs/1311.2448, 2013. [Online]. Available: <http://arxiv.org/abs/1311.2448>
- [12] Y. C. Eldar and G. Kutyniok, *Compressed Sensing: Theory and Applications*. Cambridge University Press, 2012.
- [13] S. Jokar and V. Mehrmann, "Sparse solutions to underdetermined kronecker product systems," *Linear Algebra and its Applications*, vol. 431, no. 12, pp. 2437 – 2447, 2009.
- [14] R. Vershynin, "Introduction to the non-asymptotic analysis of random matrices," *In Y. C. Eldar and G. Kutyniok (Eds.) Compressed Sensing: Theory and Applications*. Cambridge University Press. Ch. 5, 2012.
- [15] P. Stoica and P. Babu, "Sparse estimation of spectral lines: Grid selection problems and their solutions," *IEEE Trans. Sig. Proc.*, vol. 60, pp. 962–967, 2012.
- [16] N. Wagner, Y. C. Eldar, and Z. Friedman, "Compressed beamforming in ultrasound imaging," *IEEE Trans. Sig. Proc.*, vol. 60, pp. 4643–4657, Sep. 2012.